JOURNAL OF APPLIED ELECTROCHEMISTRY 22 (1992) 332–340

Electrocatalytic deposition of polypyrrole in the presence of bromide

F. BECK, M. OBERST

Universität Duisburg, Fachgebiet Elektrochemie, Lotharstrasse 1, D-4100 Duisburg 1, Germany

Received 15 March 1991; revised 25 June 1991

Bromide ions (typically $c = 1$ mM) are oxidized in acetonitrile electrolytes at platinum anodes in two steps, well separated by about 300 mV, leading to tribromoanions *1* and to bromine *2*, respectively. These basic electrochemical reactions interfere quite differently with pyrrole *3*, typically $c = 0.1$–0.01 M, added to the system. *1* oxidizes *3* to bromopyrroles, indicated by an amplification of the limiting current density of the first wave by a factor of three. No polypyrrole is deposited. In the course of the second wave, *2* oxidizes *3* to the radical cation *4*. The rate determining step in the formation of polypyrrole is a dimerization of *4* moieties, and the strong electrostatic shielding effect via complexation of *1* with *4* leads to a catalytic enhancement of the polymerization rate by more than a factor of 10 with respect to conventional systems. Regeneration of *1* in the course of these processes gives a large current amplification in the second wave. The overall reaction leads to polypyrrole, which forms an electrode coating. The material has improved properties, for example electronic conductivities above 100 S cm^{-1}. The current efficiency is nearly 100%, but only if the convection is weak. This 'negative stirring effect' is discussed in detail.

1. Introduction

Doped polypyrrole films can be obtained by anodic electropolymerization of pyrrole. The introduction of acetonitrile as an electrolyte solvent by Diaz *et al.* [1–3] yielded polymers with highly improved quality, for example in terms of electronic conductivity, over prior art electrodeposition from aqueous electrolytes [4, 5]. However, current densities were limited to impractically low values, $j < 1$ mA cm^{-2}, and a strong demand for a higher rate of electrodeposition arose. It can be foreseen that only homogeneous electrocatalysis makes sense, for a heterogeneous electrocatalyst at the anode surface would be buried by the growing polymer film in the early stages of the process. We have previously reported the possibility of an electrocatalytic formation of polypyrrole layers in the presence of bromide ions [6, 7]. The aim of this paper is to describe this case of an electrocatalysis in greater detail and to present some novel conclusions. Bromide is employed in catalytic concentrations, typically 1 mM, in the presence of conventional electrolytes like $LiClO_4$ or NBu_4BF_4. NEt_4Br does not work as supporting electrolyte in acetonitrile [8]. However, bromide electrolytes are compatible with aqueous electrolytes [9, 10]. Chemical doping with bromine vapour [11] and chemical polymerization with dissolved bromine [12, 13] is very well known. As bromine is known to react chemically with the heterocyclic nucleus, the question arises, if the backbone of polypyrrole may be modified in this way. This problem will be consequently analysed.

2. Experimental details

Pyrrole (Merck, zur Synthese) was freshly distilled (1 bar, N_2). Acetonitrile (Merck, zur Synthese) was used as such. Small amounts of water were added to adjust a water concentration of 50 mM (control by Karl Fischer Titration). NBu_4BF_4 (Fluka, purum) and $LiClO_4$ (Merck, AnalaR grade) were employed as electrolyte (0.1 M). NBu_4BF_4 contained about 1–2 mM Br^- according to voltammetric analysis (*cf.* section 3.1). It was quantitatively removed according to the following procedure: 50 g of the crude commercial product were dissolved in 50 ml 96% ethanol. 200 ml water were added slowly under stirring. The precipitate was filtered off and washed thoroughly with 200 ml EtOH/H_2O 1 : 4 (v : v). The yield (after drying, 50° C, 0.02 bar, 4 h) was about 80%. The Br^- content was reduced to about 0.1 mM. After a second purification step, a further decrease to about 0.01 mM was accomplished. Bromide was added as a catalyst by admixing NBu_4Br in concentrations of 1–10 mM.

Platinum anodes were used as substrates throughout. The cylindrical electrode was a 1 mm platinum wire, sealed in a glass tube, with a small glass globe at the lower end. The rotating disc electrode (RDE) was from PINE. Both had a surface area of 0.5 cm^2. The rotating ring disc electrode (RRDE) was also from PINE. For preparative electrodeposition, sheets of 0.1 mm platinum were employed, $A = 30$ or 42 cm^2, contacted with a brass holder well above the electrolyte level. Pretreatment of RDE and RRDE was mechanical by polishing at a rotating textile disc with diamond paste, 1 μm (Wirtz). The other platinum

0021-891X/92 © 1992 Chapman & Hall

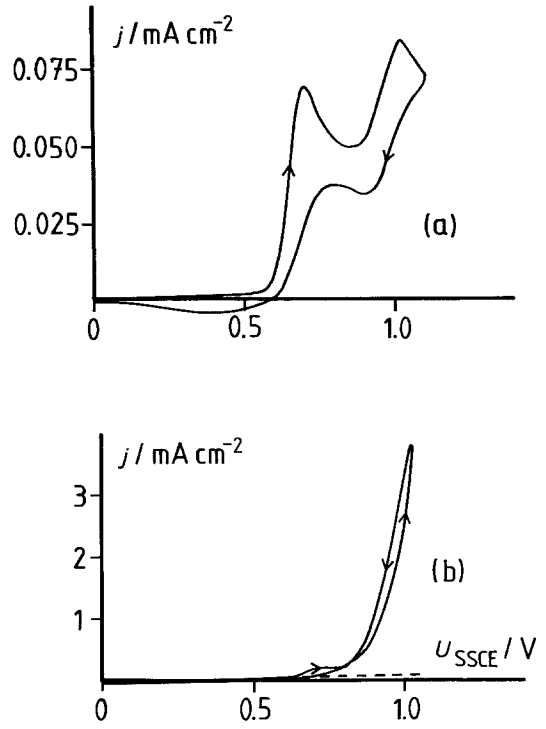

Fig. 1. Cyclovoltammetric response at Pt in a non stirred electrolyte, containing 0.1 M NBu_4BF_4 in MeCN. The supporting electrolyte was from Fluka, 'purum'. It was contaminated with 1.3 mM bromide. Voltage scan rate $v_S = 5\,mV\,s^{-1}$. (a) Without pyrrole; (b) in the presence of 0.1 M pyrrole. ---- Basic curve.

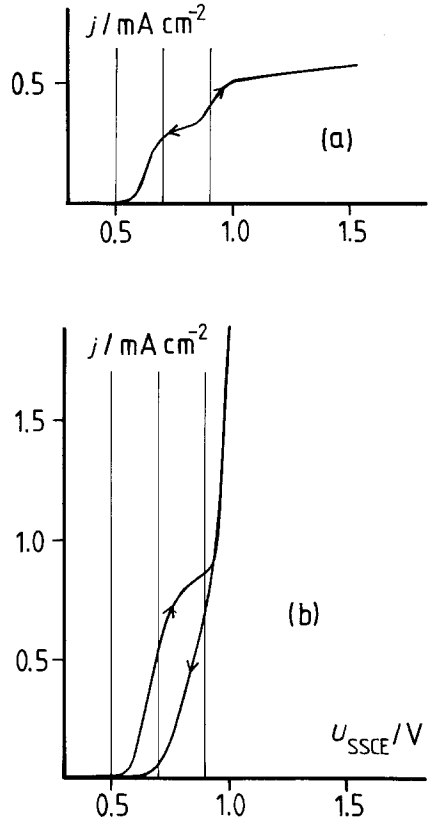

Fig. 2. Potentiodynamic oxidation of bromide (c = 1 mM NBu_4Br) in 0.1 M $LiClO_4$ in MeCN at the rotating Pt disc electrode (200 r.p.m., $5\,mV\,s^{-1}$). (a) Basic curve; (b) in the presence of 0.01 M pyrrole.

electrodes were chemically pretreated as described elsewhere [14]. The reference electrode was a saturated NaCl calomel electrode. Potentials measured against this electrode are denoted as U_{SSCE} and are + 236 mV/SHE.

Potentiodynamic measurements were performed with a potentiostat HEKA PG 284 with integrated voltage sweep generator and coulometer, in conjunction with an XY-recorder (Hewlett Packard 7046 b). A bipotentiostat (PINE, RDR3) was employed for the measurements at the RRDE.

3. Results

3.1. *Cyclic voltammetric characterization*

The wet acetonitrile/supporting electrolyte systems frequently employed in the electrodeposition of polypyrrole according to Diaz *et al.* [1–3] exhibit (in the absence of pyrrole) a characteristic voltammogram in the unstirred electrolyte with two anodic peaks, if traces of bromide are present. Figure 1a displays a characteristic example, where an electrolyte with 0.1 M NBu_4BF_4 (Fluka, purum) was employed, which contained, accidentally 1.3 mM Br^-. The peak heights are in the ratio of 2:1. No voltammetric response is obtained in the clean basic electrolyte with no bromide. The second peak behaves reversibly, the first one not. The peak current density of the first anodic peak was used for a quantitative determination of the bromide concentration, for it was found to be exactly proportional to the concentration of the bromide ions in the range 0.1–10 mM, *cf.* section 2. As quaternary ammonium perchlorates and tetrafluoborates are generally prepared by double conversion of the quaternary ammonium bromides with the sodium salts, for example

$$NR_4Br + NaBF_4 \longrightarrow NR_4BF_4\,(\downarrow) + NaBr \quad (1)$$

It is to be supposed that these salts do contain traces of bromide, if no further purification steps (*cf.* section 2) are performed. This important matter will be further discussed at the end of 3.5.

It is interesting to note a weak amplification of the first peak although a very strong enhancement of the second peak is observed in the presence of 0.1 M pyrrole, *cf.* Fig. 1b. The rereduction peaks disappear totally. Polypyrrole is electrodeposited only in the course of the more positive electrode process.

3.2. *Potentiodynamic behaviour at the rotating disc electrode*

The voltammetric measurements described in 3.1 were repeated, but under well defined mass transport conditions. Figure 2a displays the basic curve at the rotating disc electrode in the absence of pyrrole. This time 0.1 M $LiClO_4$ was used as supporting electrolyte, absolutely free of bromide, and a concentration of exactly 1 mM bromide was established by the addition of bromide. Two anodic steps are found, corresponding to the two anodic peaks in Fig. 1a. The limiting current densities are in the ratio of 2:1. The half wave potentials are roughly equal to the peak potentials in

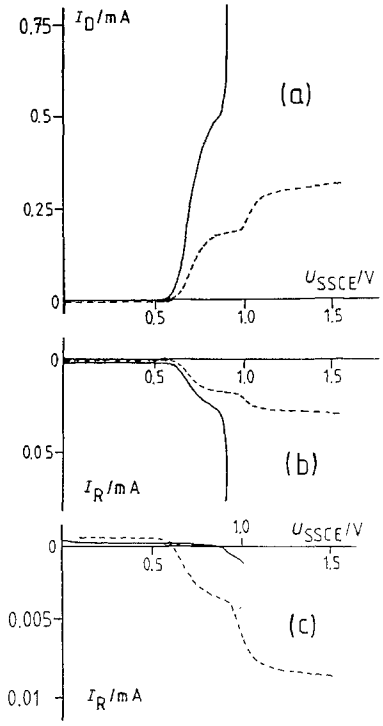

Fig. 3. Measurements at the RRDE at constant ring potential U_R(SSCE), 200 r.p.m., 5 mV s^{-1}. Electrolyte: (----) 0.1 M NBu_4BF_4, 0.05 M H_2O, 1 mM NBu_4Br in MeCN (basic electrolyte); (——) Basic electrolyte with 0.1 M pyrrole. (a) Voltammetric curves at the disc, (b) ring currents for a ring potential, held constant at $U_R = -1$ V, and (c) as (b), but $U_R = +0.2$ V.

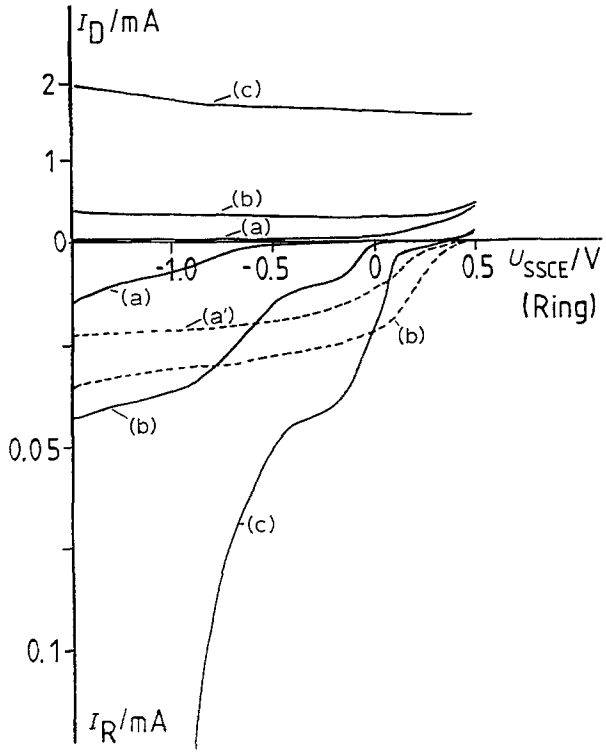

Fig. 4. Measurements at the RRDE at constant disc potentials U_D(SSCE), at 200 r.p.m., 5 mV s^{-1} Electrolyte: (----) 0.1 M NBu_4BF_4, 0.05 M H_2O, 1 mM NBu_4Br in MeCN (basic electrolyte); (——) basic electrolyte with 0.1 M pyrrole. For the lower part, U_D/V: (a') 0.7, (a) 0.8; (b) 0.9 and (c) 1.0.

Fig. 1a. Analogous curves were already depicted in our previous papers [6, 7], but with 0.1 M NBu_4BF_4 and 9 mM Br^- in MeCN.

Again a weak amplification of the negative step (1) in the presence of 0.01 M pyrrole, but a large amplification (> 10 fold) in the course of the positive process (2), (*cf.* Fig. 2b) is observed. No polypyrrole is found for step (1), but a black polypyrrole layer is electrodeposited along part (2) of the potentiodynamic curve. On changing the bromide ion concentration or the rotation speed, the two anodic reactions in the basic curve Fig. 2a are shown to be purely diffusion controlled, but not the negative wave (1) in Fig. 2b. This will be further discussed in 4.2. If the water concentration is changed, the basic curve in Fig. 2a retains its character over a wide range from 0.01 to 1 M H_2O. It is only at higher water concentrations, or in aqueous electrolytes, that one single electrode process $2Br^-/Br_2$ can be observed.

3.3. *Rotating ring disc electrode experiments*

Two measurements were made at the rotating ring disc electrode to collect more information about the nature of the electrocatalytic process. The electrode material was platinum for both electrodes. The calibration of the electrode system under the present conditions is described elsewhere [15].

Figure 3 shows a typical result for the case, where the disc potential was scanned between 0 and 1.5 V (a) and the ring potential was kept constant at two negative potentials (b, c). Clearly, the basic curve (dotted line) leads to a symmetric response at the ring. But the curve in the presence of pyrrole only leads to an analogous symmetric response, if the ring potential is relatively negative.

Interestingly, the ring current rises steeply in the region, where polypyrrole is electrodeposited at step 2 of the disc curve. Thus, soluble side products must be generated under these conditions, and rereduced at the ring. If the ring is kept at 0.2 V, the rereduction is not possible.

On the other hand, if the disc potential is kept constant and the ring is monitored between 0.5 V and −1.5 V, the potential/ring current curves displayed in Figs 4 and 5 are obtained. In the basic curve, rereduction of the disc species starts at 0.5 V. In the presence of pyrrole, other cathodic processes, starting at 0 V and at −0.5 V, can be observed. A comparison of Figs 4 and 5 discloses similar behaviour for NBu_4BF_4 and $LiClO_4$. The i_R/i_D ratios for the first limiting ring currents are essentially the same.

3.4 *Preparative electrodeposition of polypyrrole films*

Polypyrrole films were electrodeposited on the platinum sheets at current densities in the range 1–10 mA cm^{-2}. The electrolyte contained 1 mM Br^- as a redox catalyst. The nominal thickness was calculated according to [14]. The PPy layers were leached in boiling methanol for 1/2 h after the electrodeposition. The current efficiency (c.e.) was determined directly by gravimetry (semimicrobalance Sartorius R 160 P). Table 1 shows the results. At low current densities, high c.e.'s are

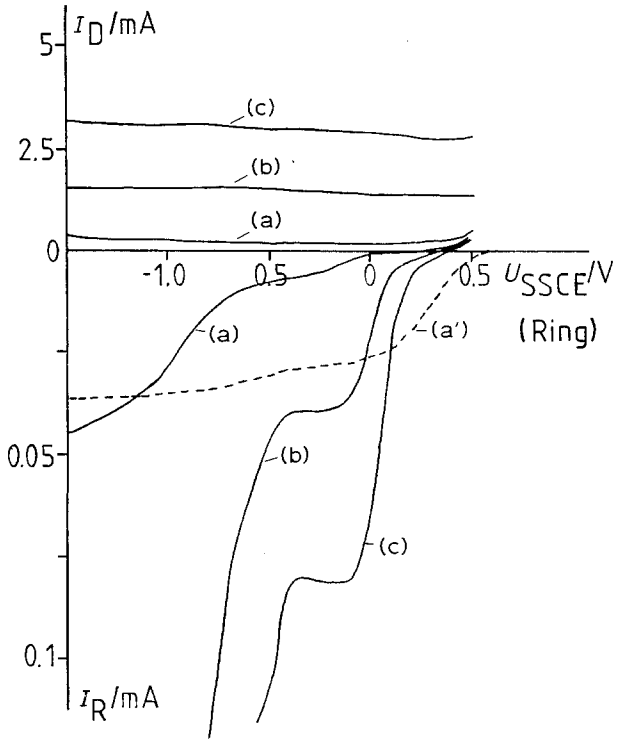

Fig. 5. The same as in Fig. 4, but with 0.1 M $LiClO_4$ as supporting electrolyte.

obtained. The reduced value at 10 mA cm^2 can be compensated by higher bromide concentrations (Nos. 1–4). Entries 5–7 demonstrate, that lower c.e.'s are found in the absence of the catalyst, especially at high c.d.'s. The water content does not hamper the process up to 0.3 M (Nos. 8–10). Table 1 finally shows that $LiClO_4$ leads to the same results and a purely aqueous system is possible.

Table 2 gives information about the bromine concentration in the polypyrrole foils. It is about 5 mol % for c = 1 mM and does not change after two galvanostatic discharge/charge cycles in an electrolyte free of bromide and pyrrole. It increases slowly with

Table 1. Electrodeposition of polypyrrole at constant current densities from acetonitrile containing 0.1 M pyrrole, 0.1 M supporting electrolyte (S.E.) and 1 mM Br^-. 23° C, very slow stirring, d_n = 10 µm, 100 mM H_2O

No.	j/mA cm^{-2}	S.E.	C.E./%	Notes
1	1	NBu_4BF_4	97	–
2	3	NBu_4BF_4	94	–
3	10	NBu_4BF_4	45	–
4	10	NBu_4BF_4	81	5 mM Br^-
5	1	NBu_4BF_4	94	no Br^-
6	3	NBu_4BF_4	89	no Br^-
7	10	NBu_4BF_4	12	no Br^-
8	2	NBu_4BF_4	96	30 mM H_2O
9	2	NBu_4BF_4	97	300 mM H_2O
10	2	NBu_4BF_4	27	10 M H_2O
11	1	$LiClO_4$	95	–
12	2	$NaBF_4$	87	Aqueous electrolyte 1 mM NaBr

Table 2. Bromine concentration, x, in polypyrrole $C_4H_3NA_{0.3}Br_x$. A = anion from supporting electrolyte after electrodeposition from bromide containing electrolytes (0.1 M pyrrole, 0.05 M H_2O, 0.1 M NBu_4BF_4 in CH_3CN). 23° C, very slow stirring, d_n = 10 µm

No.	Electrodeposition		Br in PPy x	Notes
	j/mA cm^{-2}	c_{Br^-}/mM		
1	2	1	0.05	
2	2	1	0.05	(a)
3	2	3	0.10	
4	2	5	0.15	
5	2	10	0.22	
6	10	1	0.10	
7	2	1	0.07	(b)
8	1	1	0.06	(c)
9	2	1	0.05	(d)

(a) After two galvanostatic discharge/charge-cycles in an electrolyte free of bromide and pyrrole.
(b) 0.3 M H_2O instead of 0.05 M.
(c) $LiClO_4$ instead of NBu_4BF_4.
(d) 0.1 M $NaBF_4$/1 mM NaBr in water.

increasing bromide concentration (*cf.* entries 1–5) and with current density (no. 6). A change in water concentration (No. 7), supporting electrolyte (no. 8) and solvent (no. 9) does not change the bromine content of the polymer appreciably.

Figure 6 displays the influence of the convection on the current efficiency for the electrodeposition process. The amount of polypyrrole is characterized indirectly by the redox capacity of the polymer layer, which was measured at the stationary disc. The distribution of the material at the platinum disc is shown qualitatively.

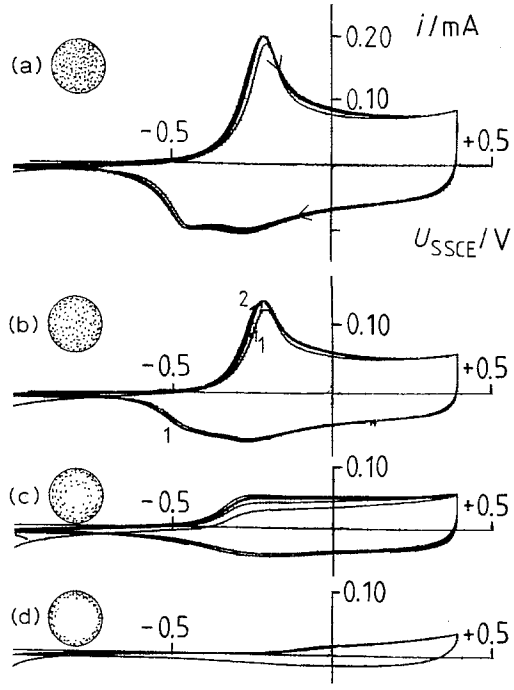

Fig. 6. Galvanostatic electrodeposition of polypyrrole at the rotating disc electrode (Pt, A = 0.5 cm^2, j = 4.5 mA cm^{-2}, t = 20 s, Q_0 = 90 mC cm^{-2}, 0.1 M NBu_4BF_4, 50 mM H_2O, 1.3 mM NBu_4Br, 0.1 M pyrrole). Rotation speeds f/r.p.m.: (a) 200, (b) 500, (c) 1000, (d) 2000. Shown are the subsequent cyclovoltammetric switching curves in the pyrrole free electrolyte at the stationary disc, v_S = 20 mV s^{-1}.

It was found, that convection has a negative effect on the current efficiency for electrodeposition ('negative stirring effect'). Curve (a) corresponds roughly to a current efficiency of 50% for the electrodeposition process.

3.5. *Further characterizations of the polypyrrole films*

Scanning electron micrographs (SEM) are shown in Fig. 7. The typical cauliflower structure can be seen at the electrolyte surface, which is quite similar to the finding in non-catalyzed systems as shown, for example, in [14]. The film surface at the backside, originally adjacent to the platinum, is very smooth. The only features are due to the scratches in the metal surface.

A much more globular texture was obtained after electrodeposition from the aqueous electrolyte containing traces of bromide. The backside is of a spongy nature. This may indicate, that the globes are hollow.

The d.c. conductivity of the free standing PPy-films was measured using a four point probe. Surprisingly, the specific conductivities were higher by a factor of nearly 3, if the material was electrodeposited in the presence of bromide. The steady state values were the following (the figures for uncatalyzed electrodeposition in parenthesis): BF^--doping: $\kappa = 146\ (50)\ S\,cm^{-1}$ and ClO_4^--doping: $\kappa = 169\ (60)\ S\,cm^{-1}$. This effect is attributed to an improved molecular order in the material; for some details see [16, 17]. In addition, strong temporary enhancement of κ was found after leaching in boiling methanol, as described below.

I.r.-spectroscopy, after the IRRAS method [18, 19], does not reveal any differences between the catalyzed and the uncatalyzed samples, if the current density was low ($0.5\,mA\,cm^{-2}$). However, at $10\,mA\,cm^{-2}$, pronounced overoxidation features (carbonyl bands [20]) appear for the uncatalyzed deposition, while the foils electrodeposited in the presence of bromine retain the undisturbed characteristics.

Large differences between the nominal thickness d_n and the real thickness d, measured after the jump method with the aid of a profilometer [21] reveal, that a high degree of porosity, P, is present. The following values are derived for BF_4^--doped polypyrrole layers ($d_n = 10\,\mu m$): $P = 50\,(29)\%$ (uncatalyzed) and $P = 16\,(0)\%$ (catalyzed). Figures in brackets correspond to layers after 30 min leaching in boiling methanol. The lower figures for the catalyzed material are chracteristic for a denser structure.

The *redox capacity* for a polypyrrole layer with a nominal thickness of $d_n = 1\,\mu m$ is found to be $Q_{redox} = 43\,mC\,cm^{-2}$, if the electrodeposition is performed at current densities in the range of $1\text{–}10\,mA\,cm^{-2}$. As the overall charge for electrodeposition is $Q_0 = 370\,mC\,cm^{-2}$ in this case, a degree of insertion of $y = 0.26$ is found, using the relationship for long chains

$$y = \frac{2Q_{redox}}{Q_0 - Q_{redox}} \qquad (2)$$

However, at lower current densities, Q_{redox} drops dramatically, *cf.* Fig. 8.

This must be discussed with respect to the prewave (1) in Figs 1 and 2, where no polypyrrole is electrodeposited. Quite the opposite behaviour is found in the absence of bromide, high efficiencies are found at low current densities, and they decrease distinctly at current densities higher than $1\,mA\,cm^{-2}$ [21]. The potential remains in the region of this prewave, and shifts at higher c.d.'s to the more positive values in the region of the main branch (2).

A typical cyclovoltammetric *redox profile* is shown in Fig. 9. It is due to a polypyrrole film, $d_n = 1\,\mu m$, which was electrodeposited in the presence of bromide. Two reduction peaks are displayed, in contrast to the voltammogram of a film electrodeposited in the absence of bromide, *cf.* Fig. 5, in our previous paper [21]*, where only one featureless reduction peak can be seen.

The presence of two reduction peaks is indicative of redoxcatalysis with bromide in the course of the electrodeposition process. The first voltammetric curve in Fig. 6 also shows this characteristic. In the literature [22] switching curves with these two peaks for NBu_4BF_4 as electrolyte can be found and we believe that the authors probably employed a salt which was contaminated with bromide.

3.6. *Chemical polymerization of pyrrole with bromine in MeCN*

Pyrrole can be polymerized chemically with bromine to yield polypyrrole [12, 13]. 10 mmol pyrrole and 10 mmol $LiClO_4$ were dissolved in 50 ml MeCN. A solution of 20 mmol bromine in 50 ml MeCN was added under stirring. Within 10 s, the solution turned dark green, then black. Within one hour, black polypyrrole precipitated. After filtration, rinsing with MeCN and drying, 0.890 g black polymer was isolated. Elemental analysis revealed a composition $C_4H_{3.59}N_{1.01}(ClO_4)_{0.00}Br_{0.54}$. 0.890 g corresponds to a yield of 81%. Surprisingly, no perchlorate was found in the polymer via Cl-analysis.

The oxidative electropolymerization was performed under the same conditions at a platinum anode ($j = 1\,mA\,cm^{-2}$, 0.1 M pyrrole, 0.1 M $LiClO_4$, 1 mM Br^-) In this case the black polymer coating had the composition $C_4H_{3.19}N_{1.00}(ClO_4)_{0.22}Br_{0.06}$. The chemical product contained ten times the amount of bromine.

In another chemical synthesis, where the concentration of the tribromideanion was increased appreciably, 10 mmol pyrrole and 10 mmol $LiClO_4$ were dissolved in 50 ml MeCN. A solution of 200 mmol NBu_4Br and 20 mmol bromine was

* The same voltammogram is shown in [7], but by error the legend does not contain the information that electrodeposition was performed in the presence of 1 mM bromide.

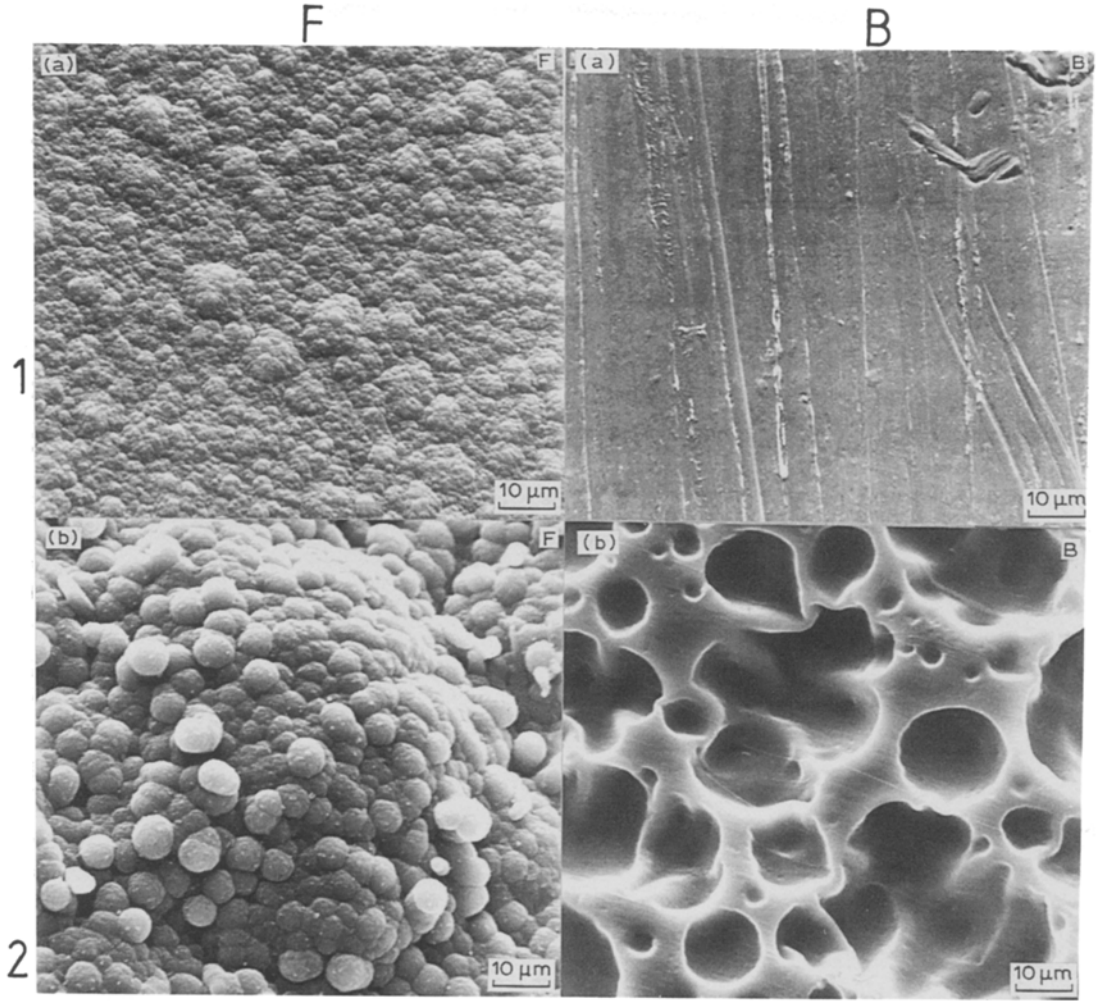

Fig. 7. SEM micrographs for d_n = 10 µm thick freestanding polypyrrole foils, electrodeposited at 2 mA cm^{-2}. (F) frontside, (B) backside. Magnification 1000 ×. Electrolyte composition: (a) 0.1 M pyrrole, 0.1 M NBu_4BF_4, 0.3 M H_2O, 1 mM NBu_4Br in acetonitrile (b) 0.1 M pyrrole, 0.1 M $NaBF_4$, 1 mM NaBr in water.

added under stirring. The colour changed much more slowly. Only after 3 hours did it become dark green. After one day, 0.0167 g of a black solid was isolated from the black solution. The presence of an excess of bromide led, therefore, to a very pronounced retardation of the polymerization process.

4. Discussion

4.1. *The bromide/bromine redox couple in acetonitrile*

According to the voltammetric measurements shown in Figs 1a and 2a, two redox processes can be distinguished for a solution of bromide in acetonitrile,

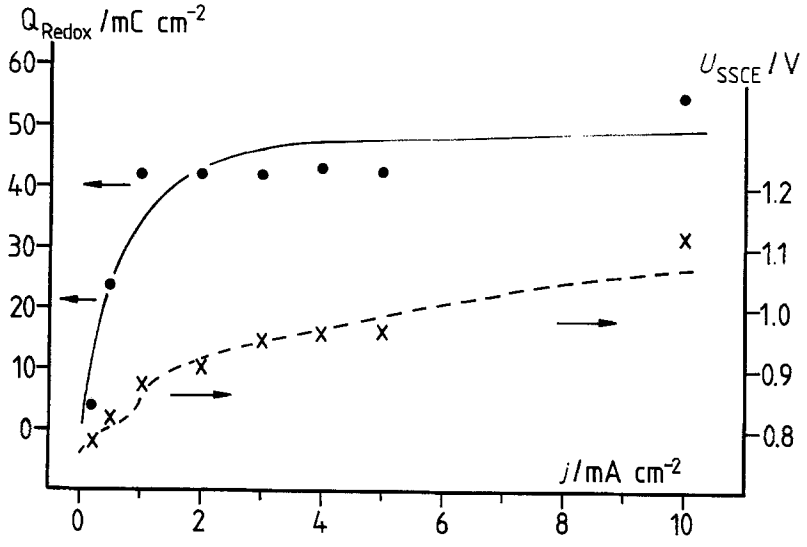

Fig. 8. Potentiodynamic redoxcapacity of galvanostatically formed polypyrrole films (d_n = 1 µm), from the standard system: 0.1 M pyrrole, 0.1 M NBu_4BF_4, 1 mM NBu_4Br, 50 mM H_2O. CV in the electrolyte free of the monomer. (●) Q_{redox} against j; (×) U_{SSCE} against j.

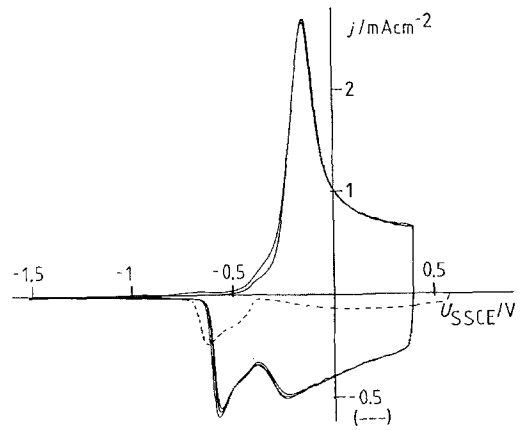

Fig. 9. Cyclovoltammetric profiles (v_S = 20 mV s^{-1}) of a polypyrrole film (d_n = 1 μm), electrodeposited at 2 mA cm^{-2} from 0.1 M pyrrole, 0.1 M NBu_4BF_4, 0.05 M H_2O, 1 mM NBu_4Br in MeCN. This cyclic curve was measured in the basic electrolyte, free of bromide. The dotted line represents the first discharge at 2 mV s^{-1}. Shown are the first five cycles of the CV-experiment.

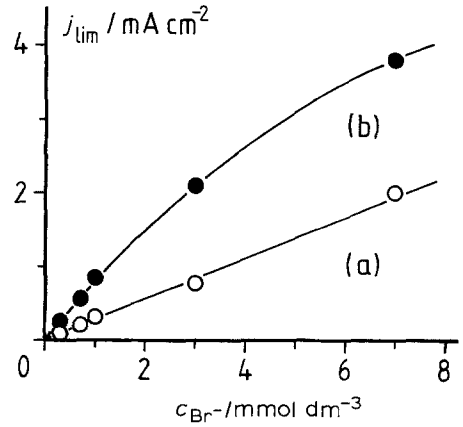

Fig. 11. A plot of limiting current j_{lim} of the first (negative) wave at the rotating disc electrode against bromide concentration c_{Br^-}. v_S = 5 mV s^{-1}, rotation speed 200 r.p.m. Basic electrolyte: 0.1 M $LiClO_4$, 0.05 M H_2O, c_{Br^-} bromide in MeCN. (○) From basic electrolytes, as above; (●) from basic electrolytes, as above, but with 0.01 M pyrrole in addition.

well separated by about 300 mV. The ratio of charges transferred in steps 1 and 2 is 2 : 1. The first (negative) process is due to the formation of the tribromoanion [23, 24]:

$$3\ Br^- \rightleftharpoons Br_3^- + 2e^- \qquad (3)$$

the tribromoanion is further oxidized to bromine in the course of the second (positive) process:

$$Br_3^- \rightleftharpoons (Br_3)^0 + e^- \qquad (4)$$

The tribromocomplex $(Br_3)^0$ appears to decompose rapidly into molecular bromine, Br_2.

Both limiting current densities involved in Fig. 2a are diffusion limited. It is demonstrated in Fig. 10, curves and a_2, that j_{lim} is proportional to $\sqrt{\omega}$, where ω is the angular velocity of the rotating disc electrode. Moreover, j_{lim} is proportional to the bromide concentration, as shown in Fig. 11. It should be noted that the two step mechanism according to Equations 3 and

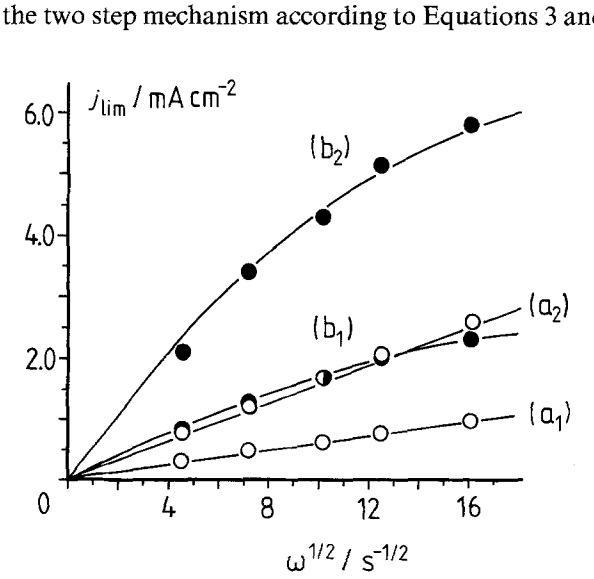

Fig. 10. A plot of limiting current densities j_{lim} of the first (negative) wave at the rotating disc electrode against angular velocity ω. Voltage scan rate v_S = 5 mV s^{-1}. Basic electrolyte: 0.1 M $LiClO_4$, 0.05 M H_2O, 1 mM Br^- (----, a_1, b_1) and 3 mM Br^- (——, a_2, b_2) in MeCN. (○) From basic electrolytes, as above; (●) from basic electrolytes, as above, but with 0.01 M pyrrole in addition.

4 is simplified to a one step redox process

$$2\ Br^- \rightleftharpoons Br_2 + 2e^- \qquad (5)$$

in aqueous solutions. Depending on the pH, complications arise due to hydrolysis of bromine. Interestingly, the two step mechanism is retained in MeCN/H_2O mixtures up to high water concentrations, *cf.* section 3.2.

4.2. *Interaction with pyrrole in the course of the negative bromide/bromine redox process*

An amplification of the first (negative) limiting current density for bromide oxidation is observed, if pyrrole is present in the electrolyte, *cf.* Figs 1b and 2b. The factor is three at low rotation speeds, ω, at the RDE and at higher bromide concentrations c_{Br^-}, but it is lowered at higher ω and c_{Br^-}, as verified in the curves $10b_1$, $10b_2$ and 11b. The reason for this is a chemical follow up reaction between Br_3^- and the pyrrole. From the current multiplication factor 3, a *substitution mechanism* is postulated. If PyH is pyrrole, with an extra labelling of one of the three different hydrogens, 1-H, 2- or 5-H and 3- or 4-H, the overall mechanism is

$$3\ Br^- + 3\ PyH \longrightarrow 3\ PyBr + 3H^+ + 6e^- \qquad (6)$$

In comparison to Equation 3, a factor of 3 is gained in the charge transfer. A substitution in the 3-position due to chemical grounds is supposed [25, 26], but a final decision is only possible via product analysis. It is known, that electrophilic substitution of pyrrole is normally directed into the 2-position, but bulky groups such as t-butyl [27] or triisopropylsilyl [28] at the nitrogen yield a high amount of 3-substitution products. In the present case, adsorption at the platinum anode may play the role of the above mentioned bulky moieties. A pure *addition mechanism* (bromine to the C=C-double bond in pyrrole), is not possible, for in this case a factor of only 1.5 would be observed

in comparison to the basic curve Equation 3

$$3\ Br^- + 1.5\ PyH \longrightarrow 1.5\ PyHBr_2 + 3e^- \quad (7)$$

The overall reaction (6) can be easily split into an electrochemical step according to Equation 3 and a chemical reaction occuring in the vicinity of the anode, e.g.

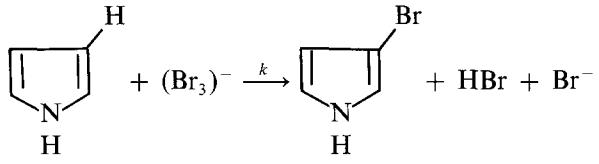

(8)

In principle, k can be evaluated via electrode kinetic procedures described in the literature [29–31], via analysis of the shift of the half wave potential. However, as the process in the course of the first wave has more or less the character of a side reaction, this was not investigated in greater detail. The RRDE experiments in Figs 4 and 5 prove the total consumption of the $(Br_3)^-$ by reactions of the type in Equation 8, and no rereduction is possible at the ring, for the cathodic response only starts at 0 V.

The decrease of the current factor to less than three at high rotation speeds may be due to the fact that the reaction layer thickness, ρ, becomes of the order of the diffusion layer thickness, δ, and some $(Br_3)^-$ species escape into the bulk of the electrolyte.

4.3 *Formation of polypyrrole in the course of the positive bromide/bromine redox process*

It is only in the course of the second step of the bromide/bromine redox couple, that pyrrole is polymerized to a black polymer establishing a polymer coating at the platinum anode. As previously pointed out [6, 7], a homogeneous redox catalysis with (Br_3) as redox mediator is assumed. In the electrochemical step (Equation 4), Br_3 is generated. In a subsequent chemical step electron transfer occurs from a pyrrole molecule to yield the radical cation and Br_3^- is regenerated

$$(Br_3) + PyH \rightleftharpoons (Br_3)^- + (PyH)^{\cdot +} \quad (9)$$

However, the direct formation of the pyrrole radical cation cannot be excluded as the potential of the (Br_3)-formation according to Equation 4 is the same as for Reaction 10:

$$PyH \longrightarrow PyH^+ + e^- \quad (10)$$

Py^+ will complex readily with the highly polarized Br_3^--anions, and the same will be the case for the dimeric dications. The formation of neutral and positive complexes A and B arises:

$$[PyH^+(Br_3)^-]^0\ (A) \text{ and } [PyH \cdot {}^{2+}_{2}\ (Br_3)^-]^+\ (B)$$

These steps occur in the adsorbed state, and they lead to an appreciable enhancement of the rate determining dimerization of the radical cations Py^+ to the dimer due to shielding of the electrostatic repulsion forces [21]:

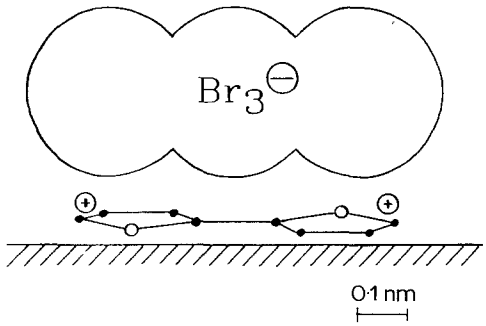

Fig. 12. Schematic representation of two (adsorbed) pyrrole radical cations, complexed by a tribromoanion, which shields the two positive charges.

$$2\ PyH^+ \xrightarrow{rds} Py\text{–}Py + 2H^+ \quad (11)$$

The molecular configuration is schematically depicted in Fig. 12.

Thus the catalytic effect is mainly due to an improved shielding effect by the large and highly polarizable anion Br_3^-, in comparison to the other anions such as BF_4^- and ClO_4^-.

These complexes do not remain exclusively at the anode surface. They may have some mobility, and in the RRDE experiment they may reach the ring cathode. This explains the pronounced cathodic currents observed in Figs 4 and 5. The wave beginning at about 0 V is due to the reduction of protons generated in processes like Equation 11, as pointed out previously in 15:

$$2\ H^+ + 2\ e^- \longrightarrow H_2 \quad (12)$$

The processes, starting at about -0.5 V, can be assigned to the rereduction of the complexes mentioned above. (A) consumes one electron and (B) two. The 'negative stirring effects' shown in Fig. 6 demonstrate that even at 200 r.p.m. PPy is formed with a current efficiency of only 50%.

Audebert and Bidan have reported the self-polymerization of various mono- and dibromopyrroles [32] and have prepared solutions of these species chemically. Polymerization to a black polymer occurs spontaneously in concentrated solutions. The authors assume a mechanism similar to that of Smith [33, 34]. Polypyrroline species are formed via proton catalysis and rearomatization occurs via HBr-elimination. The question arises, if in the present case such a mechanism could be valid. The first step would be the formation of bromopyrrols by substitution. Such a possibility is believed to be not feasible due to the following arguments:

(i) The rate of the chemical steps in the proposed present mechanism is much higher than the allowable rate, following from [32].

(ii) PPy would be generated at the first (negative) wave.

(iii) Bromine concentration in the polymers in this paper is much lower (5 mol %) than the 30–90 mol % reported in [32].

(iv) Yields in this work are near 100% and are much higher than the 20–50% found in [32].

(v) Our polypyrrole has specific conductivities well above 100 $S\,cm^{-1}$ in contrast to the 5-0.003 $S\,cm^{-1}$ reported in [32].

(vi) Bromopyrroles may not be rereduced at -0.5 V.

5. Conclusions

The anodic electropolymerization of pyrrole in the presence of catalytic amounts of bromide ions, typically 1 mM Br^-, can be accomplished with a rate enhanced by more than a factor of 10. While current densities in the uncatalyzed conditions [1, 2] are in the order of 0.5 $mA\,cm^{-2}$, the addition of 1 mM Br^- allows rates of electrodeposition of typically 10 $mA\,cm^{-2}$. The practical implications, for example for the electrochemical manufacture of PPy foils, are obvious.

The process can be explained in terms of homogeneous redox catalysis. The only other example, reported so far by Zinger [35], is based on a quinoid catalyst, tiron = 4,5-dihydroxy-1,3-benzenedisulfonic acid. The system is operative in aqueous electrolytes. Bromide catalysis can be accomplished as a clean main reaction, without any side reactions in the course of the first (negative) voltammetric wave. Such side reaction would generate monomeric products of bromination. This is due to the fact, that the main branch in the second (positive) voltammetric wave can be extended in the backward scan down to very low current densities, as demonstrated in Fig. 2b. The redox step according to Equation 4 then governs the whole range of the voltammetric curve for polypyrrole electrodeposition. The 'negative stirring effect', which is observed in experiments such as those in Fig. 6, is a consequence of soluble pyrrole intermediates in the course of the redox catalysis in the main branch rather than an effect of the participation of the stirring dependent negative prewave to the overall process. This was pointed out in detail in section 4.3.

As a consequence, the process must be performed at low stirring rates. The main branch is attained rapidly under such conditions at 10 $mA\,cm^{-2}$, and the losses mentioned above are at a minimum. Table 1 shows, that nearly quantitative current efficiencies are realizable. As demonstrated in Table 2, the bromine content in the polymer is low, in the order of 5 mol %, much lower than in other systems containing bromide [9, 32].

Acknowledgements

Financial support of our work by Arbeitsgemeinschaft Industrieller Forschungsvereinigungen (AIF) and by the German Israeli Foundation (GIF) is gratefully acknowledged. Dipl.-Ing. R. Michaelis of this laboratory has provided porosities quoted in section 3.5.

References

[1] A. F. Diaz, K. K. Kanazawa and G. P. Gardini, *J. Chem. Soc., Chem. Commun.* (1979) 635.
[2] K. K. Kanazawa, A. F. Diaz, R. H. Geiss, W. D. Gill, J. F. Kwak, J. A. Logan, J. F. Rabolt and G. B. Street, *ibid.* (1979) 854.
[3] A. F. Diaz, *Chem. Scripta* **17** (1981) 145.
[4] R. Steude, PhD-Thesis Technische Hochschule Munich (July 1933).
[5] A. Dall'Olio, Y. Dascota, V. Varacca and V. Bocchi, *C. R. Acad. Sci., Ser. C.* **267** (1968) 433.
[6] M. Oberst and F. Beck, *Angew. Chem.* **99** (1987) 1061, *Angew. Chem. Internat. Ed. Engl.* **26** (1987) 1031.
[7] F. Beck and M. Oberst, *Synth. Met.* **28** (1989) C43.
[8] G. Wegner, *Angew. Chem.* **93** (1981) 352; see especially p. 368.
[9] G. Mengoli, M. M. Musiani, M. Fleischmann and D. Pletcher, *J. Appl. Electrochem.* **14** (1984) 285.
[10] S. Tokito, T. Tsutsui and S. Saito, *Chem. Lett.* (1985) 531.
[11] M. Salomon, K. K. Kanazanawa, A. F. Diaz, M. Krounbi, *J. Polym. Sci., Polym. Lett. Ed.* **20** (1982) 187.
[12] A. Angeli, Gazz. *Chim. Ital.* **46** II (1916) 279, **48** II (1918) 21.
[13] G. P. Gardini, *Adv. Heterocycl. Chem.* **15** (1973) 67.
[14] F. Beck and M. Oberst, *Makromolek. Chem., Macromol. Symp.* **8** (1987) 997.
[15] F. Beck and M. Oberst, *J. Electroanal. Chem.* **285** (1990) 177.
[16] F. Beck and M. Oberst, *Synthetic Met.*, in press.
[17] F. Beck and M. Oberst, *Ber. Bunsenges. Phys. Chem.*, in press.
[18] K. Molt. Fresenius *Z. Anal. Chem.* **31** (1984) 743.
[19] S. Pons, J. K. Foley, J. Russel and M. Serversen, in 'Modern Aspects of Electrochemistry' No. 17, (edited by J. O. M. Bockris *et al.*), Plenum, New York (1986).
[20] F. Beck, P. Braun and M. Oberst, *Ber. Bunsenges, Phys. Chem.* **91** (1987) 967.
[21] F. Beck, M. Oberst and R. Jansen, *Electrochim. Acta* **35** (1990) 1841.
[22] A. F. Diaz, J. I. Castillo, J. A. Cojan and Wen-Young Lee, *J. Electronanal. Chem.* **129** (1981) 115.
[23] M. Michlmayr and D. T. Sawayer, *J. Electronanal. Chem.* **23** (1969) 387.
[24] T. Iwasita and M. C. Giordano, *Electrochim. Acta* **14** (1969) 1045.
[25] A. Gossauer, 'Die Chemie der Pyrrole', Springer, Berlin (1974).
[26] R. A. Jones and G. P. Bean, 'The Chemistry of Pyrroles', Academic Press, London (1977).
[27] C. F. Candy, R. A. Jones and P. H. Wright, *J. Chem. Soc.* (1970) *C*2563.
[28] J. M. Muchowski and D. R. Solas, *Tetrahedron Lett.* **24** (1983) 3455.
[29] D. G. Gray and J. A. Harrison, *J. Electoanal. Chem.* **24** (1970) 187.
[30] D. Möller and K. H. Heckner, *ibid.* **38** (1972) 337.
[31] F. Opekar and P. Beran, *ibid.* **69** (1976) 1.
[32] P. Audebert and G. Bidan, *Synthetic Met.* **15** (1986) 9.
[33] H. A. Potts and G. F. Smith, *J. Chem. Soc.* (1957) 4018.
[34] G. F. Smith, *Heterocyclic Chem.* **2** (1963) 287.
[35] B. Zinger, *Synthetic Met.* **28** (1989) C37.